LINCS gene expression signature analysis revealed bosutinib as a radiosensitizer of breast cancer cells by targeting eIF4G1

SAI HU[1,2], DAFEI XIE[2], PINGKUN ZHOU[1,2], XIAODAN LIU[2], XIAOYAO YIN[3], BO HUANG[1] and HUA GUAN[2]

[1]Institute for Environmental Medicine and Radiation Hygiene, School of Public Health, University of South China, Hengyang, Hunan 421001; [2]Department of Radiation Biology, Beijing Key Laboratory for Radiobiology, Beijing Institute of Radiation Medicine, Beijing 100850; [3]College of Computer, National University of Defence Technology, Changsha, Hunan 410073, P.R. China

Received August 29, 2020; Accepted January 22, 2021

DOI: 10.3892/ijmm.2021.4905

Abstract. Radioresistance is the predominant cause for radiotherapy failure and disease progression, resulting in increased breast cancer-associated mortality. Using gene expression signature analysis of the Library of Integrated Network-Based Cellular Signatures (LINCS) and Gene Expression Omnibus (GEO), the aim of the present study was to systematically identify potential candidate radiosensitizers from known drugs. The similarity of integrated gene expression signatures between irradiated eukaryotic translation initiation factor 4 γ 1 (eIF4G1)-silenced breast cancer cells and known drugs was measured using enrichment scores (ES). Drugs with positive ES were selected as potential radiosensitizers. The radiosensitizing effects of the candidate drugs were analyzed in breast cancer cell lines (MCF-7, MX-1 and MDA-MB-231) using CCK-8 and colony formation assays following exposure to ionizing radiation. Cell apoptosis was measured using flow cytometry. The expression levels of eIF4G1 and DNA damage response (DDR) proteins were analyzed by western blotting. Bosutinib was identified as a promising radiosensitizer, as its administration markedly reduced the dosage required both for the drug and for ionizing radiation, which may be associated with fewer treatment-associated adverse reactions. Moreover, combined treatment of ionizing radiation and bosutinib significantly increased cell killing in all three cell lines, compared with ionizing radiation or bosutinib alone. Among the three cell lines, MX-1 cells were identified as the most sensitive to both ionizing radiation and bosutinib. Bosutinib markedly downregulated the expression of eIF4G1 in a dose-dependent manner and also reduced the expression of DDR proteins (including ATM, XRCC4, ATRIP, and GADD45A). Moreover, eIF4G1 was identified as a key target of bosutinib that may regulate DNA damage induced by ionizing radiation. Thus, bosutinib may serve as a potential candidate radiosensitizer for breast cancer therapy.

Correspondence to: Dr Hua Guan or Dr Dafei Xie, Department of Radiation Biology, Beijing Key Laboratory for Radiobiology, Beijing Institute of Radiation Medicine, 27 Taiping Road, Haidian, Beijing 100850, P.R. China
E-mail: ghlsh@163.com
E-mail: xiedafei@sina.com

Key words: eIF4G1, bosutinib, radiosensitization, LINCS, enrichment score, drug reposition

Introduction

Breast-conservative surgery followed by radiation therapy (RT) currently is the standard of care for breast cancer (1). Although breast-conservative surgery with RT improves overall patient survival and is universally accepted as the gold standard in breast cancer treatment. However, improved approaches targeting cancer cells that develop resistance to RT are still needed (1-3). Indeed, the appearance of radioresistant cells leads to treatment failure and local recurrence, thus requiring administration of higher doses of radiation in these areas of recurrence, which may cause damage to healthy tissues surrounding the tumor. Therefore, the identification of new pharmacological approaches that could overcome radioresistance of cancer cells is crucial (3-5).

It is well established that intrinsic and ionizing radiation (IR)-induced radioresistance determines cellular responses to RT. Previous studies have identified numerous radioresistance-associated genes, including eukaryotic translation initiation factor 4 γ 1 (*eIF4G1*) (6), insulin-like growth factor 1 receptor (*IGF-1R*) (7), CST telomere replication complex component 1 (*CTC1*) (8), and DNA-dependent protein kinase (*DNA-PK*), which may represent potential molecular targets for radiosensitization (9). DNA repair, cancer stemness, apoptosis (10), cell cycle arrest (11), autophagy (12), and hypoxia (13) have been proposed as essential biological mechanisms leading to radioresistance of cancer cells. Among the radiosensitizers under active investigation or in use are agents targeting hypoxic cells, inhibitors of ion channels (14), regulators of proteins (such as enzymes) (15-17) or pathways (18) and inhibitors of autophagy (19). However, several limitations exist with these compounds, such as lack of specificity, unclear underlying molecular mechanisms, and adverse effects (3). Moreover, there is a paucity of promising radiosensitizers for a variety of cancer types, including breast cancer.

Drug discovery, including for radiosensitizers, is both time-consuming and costly. Moreover, the design and synthesis of new compounds, along with high-throughput screening, remain challenging (20). Drug repositioning (also known as drug repurposing or drug reprofiling) allows the prediction of alternative applications for existing drugs. This strategy can help reduce the time and cost associated with new drug development and improve the delivery of new drugs to patients with severe diseases (21). Thus, drug repositioning may be a promising strategy for the identification of known compounds, such as potentially effective radiosensitizers, that could improve the efficacy and reliability of RT.

Bosutinib is a small BCR-ABL kinase inhibitor approved by the US Food and Drug Administration (FDA) in 2012 with improved tolerance and safety, compared with other tyrosine kinase inhibitors. BCR-ABL kinase plays an important role in the onset and rapid progression of chronic myelogenous leukemia and is among the primary targets of bosutinib. Other known targets include LYN, SRC, CDK2, and MAP2K1 (22,23). It has been reported that inhibition of SRC could enhance the radiosensitivity of numerous of cancer cell types (24,25). In the present study, we found bosutinib and silencing of eIF4G1 following IR had similar therapeutic effects. Bosutinib was identified as a radiosensitizer of breast cancer cells for it significantly sensitized cancer cells to DNA damage induced by RT through the regulation of cell apoptosis (26) and expression of several proteins including eIF4G1, ATM, and XRCC4. Additional experiments were carried out to examine the underlying mechanism and verify the adjuvant effect of bosutinib in breast cancer cells exposed to γ-rays. The addition of bosutinib led to an apparent radiosensitizing effect in breast cancer cells, thus allowing the use of decreased dosages of both the drug and radiation, with fewer side effects.

Materials and methods

Library of integrated network-based cellular signatures (LINCS). The cellular signatures of all compounds used in this study were collected and extracted in October 2017 from the LINCS comprehensive systems biology portal (http://www.lincscloud.org/). It is a large-scale pharmacogenomics dataset based on HDF5 file format containing cellular signatures in response to a variety of perturbations including agents, genetic mutations, micro-environments and diseases (27). The whole database of gene expression profiles of treatments and their corresponding controls in each perturbagen was downloaded from the portal in homepage of the website. We then selected 55,129 cellular response signatures of 4,617 chemical reagents at different time-points and doses and 4,388 signatures of untreated cells as controls. The signatures were extracted and integrated for identification and prediction of potential radiosensitizers in this study.

Gene expression omnibus (GEO). The raw gene expression profile dataset GSE41627 (https://www.ncbi.nlm.nih.gov/geo/query/acc.cgi?acc=GSE41627) used in this study was extracted in October 2017 from the GEO (https://www.ncbi.nlm.nih.gov/geo/) database. The GEO was scanned for gene expression profiles related to radiotherapy of breast cancer according to 2 criterions for precise match with LINCS: i) Platform GPL570 or GPL96 was employed. ii) Cell lines used should be matched accurately. GSE41627 was selected eventually, comprising expression profiles of several DNA damage response (DDR) genes in IR in human breast cancer cells. This dataset by Badura *et al* (26) reported 12 samples from 4 cell lines exposed to 10 Gy of γ-ray irradiation, with or without eIF4G1 silencing. In 'Download family' in the website, 'Series Matrix File(s)' of GSE41627 in '.txt' were downloaded for further comparison and analysis.

Calculation of enrichment scores (ES). Probe IDs in LINCS were converted into official gene symbols according to annotation files of the platform of GPL96. However, those in GSE41627 were conducted according to annotation files of the platform of GPL570. Processing of gene expression signatures from LINCS and GSE41627 was carried out using the 'contrasts. fit' function in Limma package (v3.24.14) (28) in R software (3.4.4). Cellular response data of treatment groups and their controls of the two datasets were inputted and differential expressions of the whole genome were determined after running of the scripts. The lists of all differentially expressed genes in LINCS and GSE41627 were obtained, respectively. ES were used to evaluate the similarity between the gene expression signatures of cells treated with a variety of compounds and those of irradiated, eIF4G1-silenced cells. Gene set enrichment analysis (GSEA) was performed using GSEA software (v. 3.0) (29). The gene lists of the two datasets were inputted into the software and the classic scoring scheme was used to calculate ES for the silencing and compounds in LINCS. The maximum and average ES in each case were obtained as a result.

Cell culture and irradiation. The human MX-1, MCF-7, and MDA-MB-231 breast cancer cell lines were used in this study. MCF-7 (cat. no. CL0206) and MDA-MB-231 (cat. no. CL0208) cells were purchased from the American Type Culture Collection (ATCC). MX-1 cells (cat. no. CL0456) were provided by the Beijing Institute of Transfusion Medicine and initially purchased from the ATCC.

The cells were cultured in Dulbecco's modified Eagle's medium (DMEM) supplemented with 10% FBS (Sigma-Aldrich; Merck KGaA), 100 U/ml penicillin and 100 μg/l gentamycin and incubated at 37˚C in a humidified atmosphere containing 5% CO_2. The cells were passaged once for 2 days with a total of three passages. After each resuscitation, 3-5 generations were used.

Cells were divided into four groups: i) Irradiation alone; ii) Drug alone; iii) Irradiation and drug; and iv) Control. Irradiation was carried out using ^{60}Co γ-rays at a dose rate of 1.98 Gy/min at room temperature in the Beijing Institute of Radiation Medicine. Then, 2 Gy and 4 Gy of γ-rays were used according to previous studies and the daily doses in common use in classical radiotherapy for breast cancer in clinic (30,31).

Drugs and antibodies. The drugs used in the present study included: Bosutinib (cat. no. E047103; Shanghai EFE Biological Technology Co., Ltd.), bifonazole (cat. no. B3563; Sigma-Aldrich; Merck KGaA), and isosorbide (cat. no. 652-67-5; J&K Scientific, Ltd.).

The antibodies used in immunoblotting analyses were as follows: Anti-eIF4G1 (cat. no. ab2609; Abcam; rabbit; polyclonal), anti-eIF4G2 (cat. no. 3468; Cell Signaling Technology, Inc.; rabbit; monoclonal), anti-ATM (cat. no. ab201022; Abcam; rabbit; monoclonal), anti-γH2AX (Ser139; cat. no. ab11174; Abcam; rabbit, polyclonal), anti-XRCC4 (cat. no. SC-271087; Santa Cruz Biotechnology, Inc.; mouse; monoclonal), anti-ATRIP (cat. no. ab175221; Abcam; rabbit; monoclonal), anti-GADD45A (cat. no. ab7664; Abcam; rabbit; polyclonal), anti-PARP-1 (cat. no. SC-7150; Santa Cruz Biotechnology, Inc.; rabbit; polyclonal), anti-Mre11 (cat. no. ab214; Abcam; mouse; monoclonal), anti-pCDK1-Y15 (cat. no. 9116S; Cell Signaling Technology, Inc.; mouse; monoclonal), anti-CDK1 (cat. no. ab201008; Abcam; rabbit; monoclonal) and anti-β-actin (cat. no. TA-09; Beijing Zhongshan Jinqiao Biotechnology Co. Ltd.; mouse; monoclonal).

Cell proliferation. Cell proliferation was analyzed using a Cell-Counting Kit-8 (CCK-8) assay kit (Engreen) following the manufacturer's instructions. Briefly, cells were seeded in 96-well plates and exposed to increasing concentrations of test drugs alone. To assess cell proliferation, CCK-8 solution (cat. no. CK04; Dojindo Molecular Technologies, Inc.) was added 48 and 72 h after the treatment (32,33). The absorbance was measured at 450 nm using a microplate reader. Half-maximal inhibitory concentrations (IC_{50}) were calculated using GraphPad Prism 8.0.1 (244) software (GraphPad Software, Inc.). Each experiment was performed in triplicate.

Cell viability. Cell viability was assessed using colony formation assays. Cells were seeded into 60-mm culture plates at a density of $3x10^2$ cells/plate and exposed to various concentrations of bosutinib for 24 h (34). Following irradiation, the cells were cultured in normal medium for 10-15 days. Surviving tumor cells were fixed with ethanol and stained with Giemsa, and the colonies were then counted.

Immunoblotting analyses. The cells were treated with bosutinib for 12 and 24 h (35). Total proteins were extracted from cultured cells on ice with lysis buffer supplemented with protease inhibitor cocktail. The BCA method was used for protein quantification. Cell lysates were separated using SDS-PAGE with a Bio-Rad Bis-Tris Gel system (percentages of SDS-PAGE were: 8% for ATM, XRCC4 and ATRIP; 10% for eIF4G1 and eIF4G2; 12% for γH2AX and GADD45A). Separated proteins were then transferred to PVDF membranes. The membranes were blocked with 5% non-fat dry milk at room temperature for 1 h. Subsequently, the membranes were incubated overnight at 4˚C with the primary antibodies. The antibodies used were as follows: Anti-eIF4G1 (cat. no. ab2609), anti-eIF4G2 (cat. no. 3468), anti-ATM (cat. no. ab201022), anti-γH2AX (Ser139; cat. no. ab11174), anti-XRCC4 (cat. no. SC-271087), anti-ATRIP (cat. no. ab175221), anti-GADD45A (cat. no. ab7664), anti-PARP-1 (cat. no. SC-7150), anti-Mre11 (cat. no. ab214), anti-pCDK1-Y15 (cat. no. 9116S), anti-CDK1 (cat. no. ab201008) and anti-β-actin (cat. no. TA-09). The dilutions of anti-eIF4G1 and anti-γH2AX were 1:3,000 and 1:2,000, respectively. The dilution of all other antibodies was 1:1,000. The membranes were then washed three times with TBST and incubated with the indicated secondary antibodies conjugated with HRP (1:4,000; 1 h) at room temperature. The antibodies were as follows: anti-mouse (cat. no. 140193; Jackson ImmunoResearch, Inc.) and anti-rabbit (cat. no. 138442; Jackson ImmunoResearch, Inc.). The target bands were visualized using the Image Quant LAS500 system. Densitometry analysis was conducted by ImageJ software (1.51j8).

Measurement of cell apoptosis. Cells ($3x10^5$-$6x10^5$) were treated with bosutinib for 24 h before irradiation with 4 Gy ^{60}Co γ-rays, then subjected to trypsinization with trypsin/EDTA (HyClone; Cytiva) 8, 12, and 24 h following irradiation. For apoptosis measurement, the cells were centrifuged with 179 x g at 4˚C for 3 min. The cell pellets were re-suspended in 100 µl binding buffer and stained with 5 µl propidium iodide (50 µg/ml) and 5 µl Annexin V-FITC (cat. no. DA10; Dojindo Molecular Technologies, Inc.). Apoptosis was then analyzed using a flow cytometer (ACEA Novocyte).

Immunofluorescence (IF). MDA-MB-231 cells were cultured on coverslips and treated with 4 Gy of IR. The cells were washed three times with PBS at 4˚C at 1, 4 and 8 h after IR and then incubated with 4% paraformaldehyde at room temperature for 15 min. The cells were subsequently permeabilized with PBS containing 0.5% Triton X-100 at room temperature for 10 min, and blocked with 3% of Albumin Bovine Fraction V (CAS 9048-46-8; KainuoBio) in PBS at room temperature for 1 h. Then the cells were incubated with γH2AX antibody (1:200 for IF, Ser139; cat. no. 05-636; Merck Millipore; mouse, monoclonal) for 1 h at room temperature. Cells were subsequently washed three times with PBS and then incubated with the secondary antibody (1:400, Ser139; cat. no. A11029; Invitrogen; mouse) in phosphatase at room temperature for 1 h. Then DAPI staining was performed at room temperature for 5 min. Slides were imaged using the Nikon Application for Inverted Research Microscope ECLIPSE Ti2 Series and oil immersion lens of x100 was used.

Calculation of combination indices. Combination indices (CI) of bosutinib and radiation were calculated with the tool CompuSyn (ComboSyn, Inc.) using the Chou-Talalay method based on the median-effect equation (36). It was derived from the mass-action law principle describing interactions among multiple entities and first order and higher order dynamics. Dose-effect data points of the components and combinations were input, respectively, and the resulting CI in 'CompuSyn Report' accurately indicates additive effect (CI=1), synergism (CI <1), and antagonism (CI >1) for drug combinations. This tool provided an easy and flexible approach for drug efficacy evaluation in drug combination studies.

Statistical analysis. Statistical analysis of the GEO dataset was conducted using an empirical phenotype-based permutation test procedure (29). The phenotype labels were permuted randomly, and the ES of the gene set in the gene list of fold changes for the permuted data was recomputed. The P-value of the observed ES was then calculated relative to this distribution. The number of permutations was set to 1,000, and $P<0.05$ was considered to indicate a statistically significant difference.

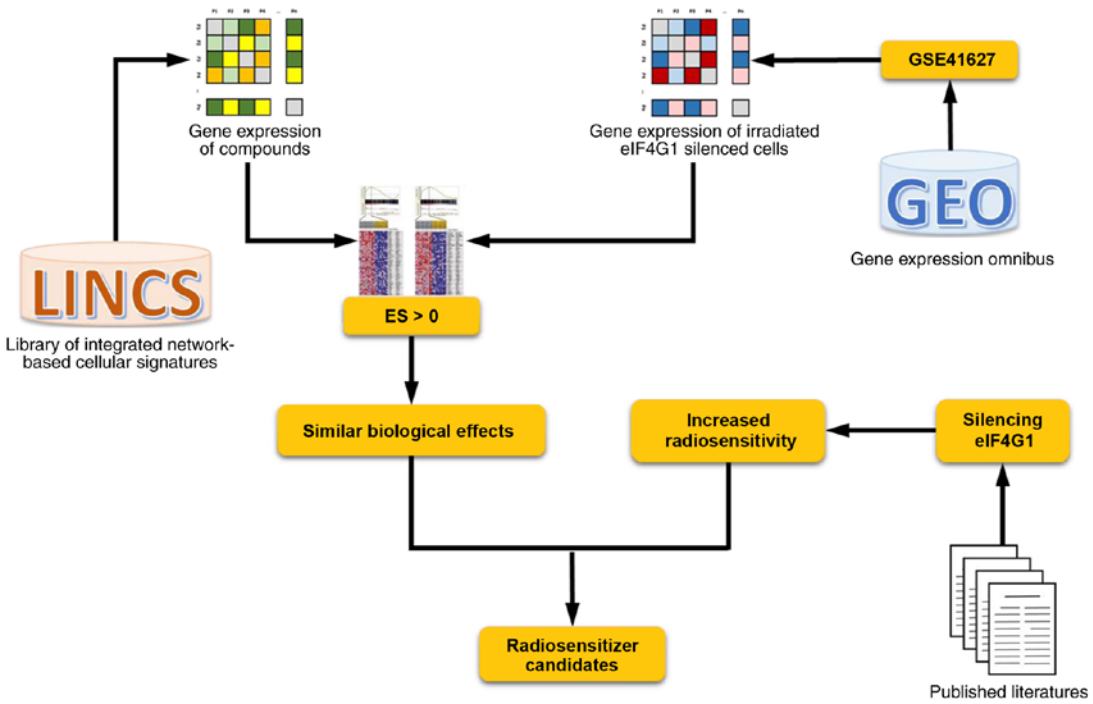

Figure 1. The schematic representation of the workflow of the approach in identification of candidate radiosensitizers. They were screened out from the Library of Integrated Network-based Cellular Signatures (LINCS) based on comparison of similarity of gene expression profiles between drug-treated and irradiated eIF4G1-silenced breast cancer cells. ES, enrichment score.

Experiments were performed at least in triplicate. Data from three or more independent experiments are presented as the mean ± SD. The data were analyzed using one-way ANOVA. Differences between two groups were analyzed using Student's t-test. Differences among four groups were analyzed using Tukey's post hoc test. Statistical analyses were performed using SPSS 18.0 software (IBM Corp.). $P<0.05$ was considered to indicate a statistically significant difference.

Results

Extraction and integration of gene expression profiles. Following screening and manual curation, the gene expression profiles from the GSE41627 dataset were selected for the identification of potential radiosensitizers. Treatment groups were divided into four groups, including irradiated cells, eIF4G1-silenced cells, irradiated eIF4G1-silenced cells, and the control group. The silencing of eIF4G1 has been shown to significantly sensitize breast cancer cells to IR. Therefore, radiosensitizer candidates were identified by comparing the biological effects of the gene expression profiles from the GSE41627 dataset and those of breast cancer cells from LINCS in response to treatment with different chemical compounds. The flow diagram is shown in Fig. 1.

Identification of potential radiosensitizers. Gene expression signatures of the GSE41627 dataset, as well as those generated from breast cancer cells treated with various compounds, were analyzed using R code. The integrated genome-wide differential expression signature lists of irradiated eIF4G1-silenced cells and compounds from LINCS were inputted and ES between -1 and 1 were outputted indicating their similarity in biological effects. A positive ES for a known compound indicates that the drug-induced profile is similar to the effect of silencing eIF4G1 in response to irradiation, suggesting that the queried compounds can increase the radiosensitivity of breast cancer cells.

A total of 2,089 entries from LINCS, including different concentrations of each drug, were evaluated. These were obtained at 96 and 144 h following eIF4G1 knockdown. The maximum and the average ES were calculated for each entry. Thresholds for screening were selected based on the ES of each compound to ensure that ≤5% of compounds were screened in each case. In total, 11 compounds were proposed as candidate radiosensitizers for consideration of further study.

For compounds examined 96 h after eIF4G1 knockdown, both the maximum and the average ES of 369 drugs were positive (Table SI). Considering 0.70 and 0.56 as thresholds for the maximum ES and average ES, respectively, two experimental drugs (SU-11652 and latrunculin-b) were selected. SU-11652 is a multi-targeting receptor tyrosine kinase inhibitor currently investigated as an anticancer drug (37). Latrunculin-b is a cell-permeable actin polymerization inhibitor against cancer (38). Considering only the drugs approved by the FDA, four drugs (floxuridine, palbociclib isethionate, raltitrexed, and bosutinib) were screened when the thresholds for maximum and average ES were set at 0.66 and 0.48, respectively.

At 144 h following eIF4G1 knockdown, 179 drugs exhibited positive maximum and average ES (Table SI). PD-0325901, an experimental MEK kinase inhibitor with marked anti-tumor activity (39) was identified with 0.49 and 0.36 as thresholds for the maximum ES and average ES, respectively. Considering only drugs that were FDA approved were used, no candidates had maximum ES and average ES above the thresholds simultaneously. Thus, we changed the thresholds ensuring <10% of the compounds would be screened. The maximum ES

Table I. Top-ranked compounds compared with irradiated eIF4G1-silenced breast cancer cells.

Drugbank ID	Pert name	Drug group	Time-point	Max ES	Ave ES
DB08009	SU-11652	[a]Experimental	96 h	0.7094	0.6366
DB08080	Latrunculin-b	Experimental	96 h	0.7043	0.5687
DB00322	Floxuridine	[b]Approved	96 h	0.6880	0.5784
DB09073	Palbociclib	Approved	96 h	0.6827	0.5613
DB00293	Raltitrexed	Approved; [c]Investigational	96 h	0.6699	0.6010
DB06616	Bosutinib	Approved	96 h	0.6616	0.5124
DB07101	PD-0325901	Experimental	144 h	0.4970	0.4006
DB00001	Lepirudin	Approved	144 h	0.5649	0.2470
DB00806	Pentoxifylline	[d]Approved; Investigational	144 h	0.4983	0.0669
DB04794	Bifonazole	Approved	144 h	0.4320	0.3882
DB01020	Isosorbide	Approved	144 h	0.3874	0.3836

[a]Experimental: A compound that has been shown experimentally to bind specific proteins in mammals, bacteria, viruses, fungi, or parasites. This includes compounds that are pre-investigational new drug applications or in discovery phase. [b]Approved: Refers to a drug that has been approved in at least one jurisdiction. [c]Investigational: Refers to a drug that is in some phase of the drug approval process in at least one jurisdiction. [d]Approved; investigational: Refers to groups for different jurisdictions of a drug.

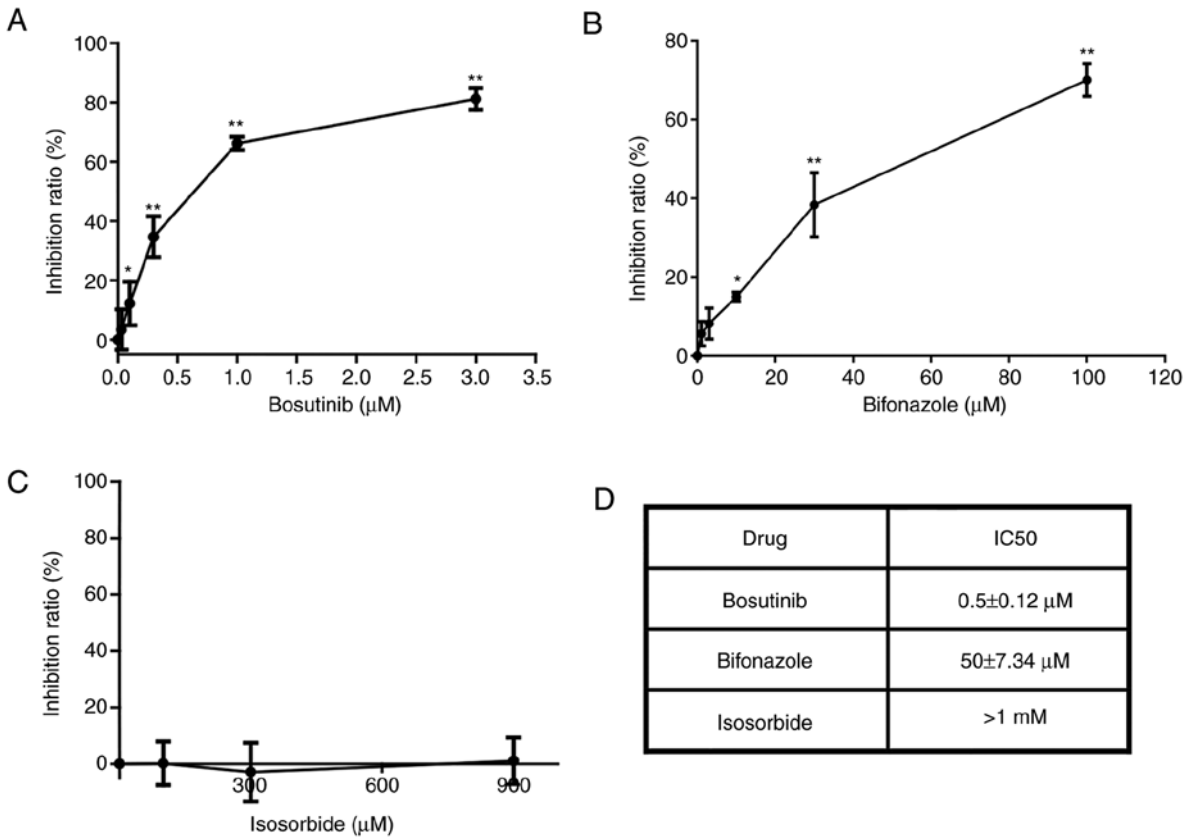

Figure 2. Cell growth inhibition and half-maximal inhibition concentration (IC_{50}) of the selected candidate drugs. MX-1 cells were treated with different concentrations of bosutinib, bifonazole, or isosorbide for 48 h. The cell growth inhibition was determined by CCK-8 assays. The DMSO solvent was used as the control. (A-C) Inhibition of MX-1 cell growth by bosutinib, bifonazole, and isosorbide. $^{*}P<0.05$, $^{**}P<0.01$. Error bars show means ± standard deviations of three independent experiments. (D) The IC_{50} of the tested drugs on cell growth. Each experiment was repeated three times.

of 10 FDA-approved drugs was >0.47, including lepirudin, pentoxifylline, and trametinib. The average ES of 14 approved drugs was >0.30, including bifonazole, isosorbide mononitrate, and anastrozole.

Selection of promising candidate radiosensitizers. The comparison of transcriptional signatures identified several candidate radiosensitizers. The selected candidates are listed in Table I. Compounds with both the maximum ES and average ES higher

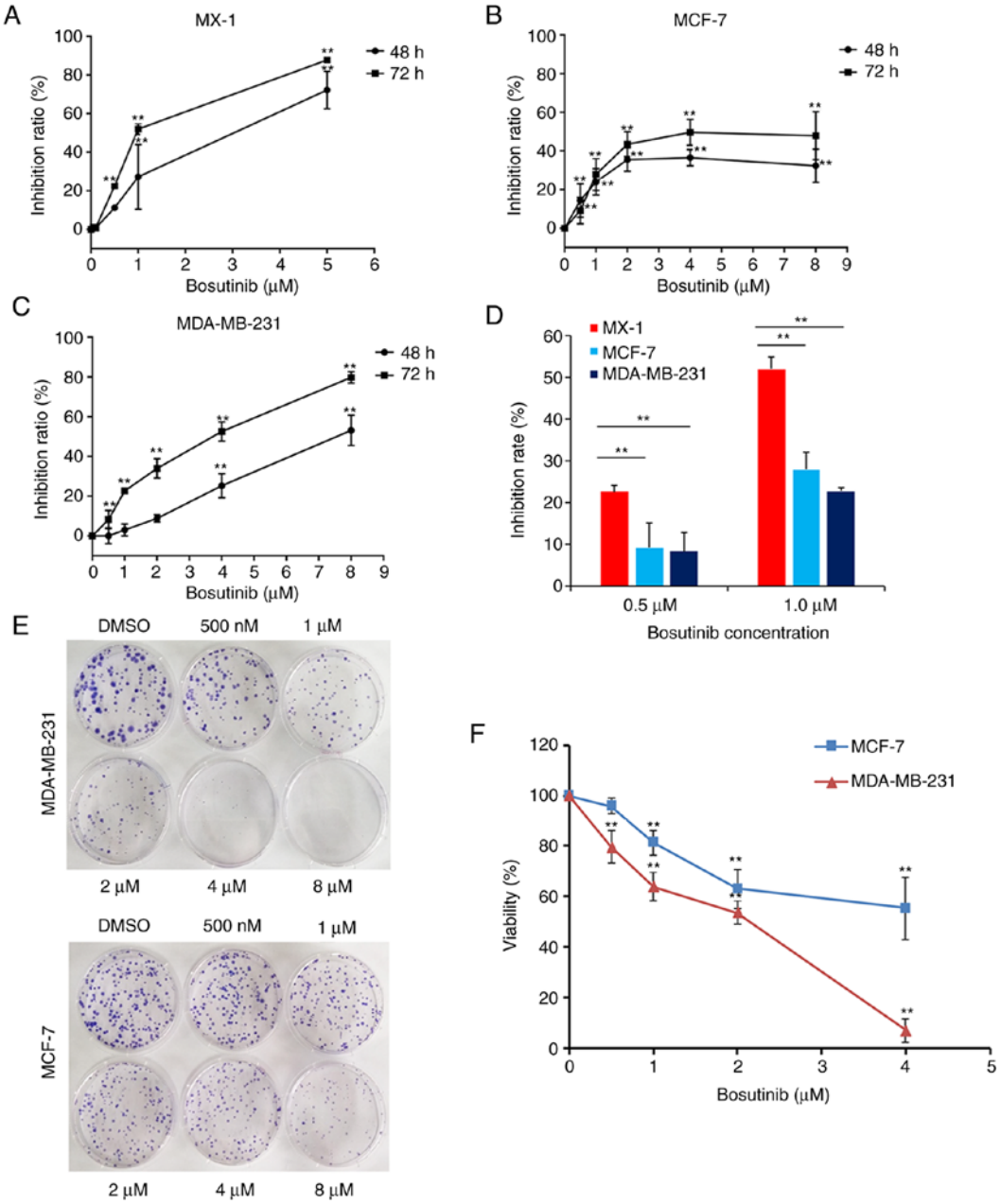

Figure 3. Effects of bosutinib on the cell growth of different cell lines. (A-C) Bosutinib inhibits the cell growth of MX-1, MCF-7, and MDA-MB-231, determined by CCK-8 assays. (D) Comparison of cell growth inhibition by bosutinib on the three tested cell lines. (E) Effect of bosutinib on colony formation of MCF-7 and MDA-MB-231 cells. (F) Cell survival of MCF-7 and MDA-MB-231 cells treated with different concentrations of bosutinib represented by cell colony-forming capability. **P<0.01. Error bars show means ± standard deviations of three independent experiments.

than thresholds were selected, except in the case of approved drugs at 144 h following eIF4G1 knockdown, as no compounds met these criteria. Therefore, the top two compounds based on maximum ES and average ES in this case were selected.

Bosutinib, bifonazole, and isosorbide were selected for further validation and additional studies on the role and mechanism of eIF4G1 in the cellular response to IR-induced DNA damage. Among them, bosutinib has been used in the treatment of Philadelphia chromosome-positive (Ph^+) chronic myelogenous leukemia with resistance or intolerance to prior therapy, according to DrugBank.

Bosutinib inhibits cell viability. The inhibitory effects of the selected candidate drugs (bosutinib, bifonazole, and isosorbide) on the viability in MX-1 cells are presented in Fig. 2. Of these, isosorbide exhibited no evident inhibitory effect at concentrations <1 mM (Fig. 2C and D). Bosutinib was more effective (Fig. 2A and B), as its IC_{50} was only 1% of that of bifonazole (Fig. 2D). Thus, bosutinib was used in subsequent experiments.

Bosutinib was used to treat MX-1, MCF-7, and MDA-MB-231 cells for 48 or 72 h. The inhibition rates changed with the concentration of bosutinib. In MX-1 and MDA-MB-231 cells, the inhibition rates markedly increased in response to bosutinib (Fig. 3A and C). However, in MCF-7 cells, although at the concentration of 2 μM, the inhibition rates of bosutinib were even higher than that in MDA-MB-231 cells, this was only the case at concentrations <4 μM of bosutinib, and higher concentrations had no effect (Fig. 3B).

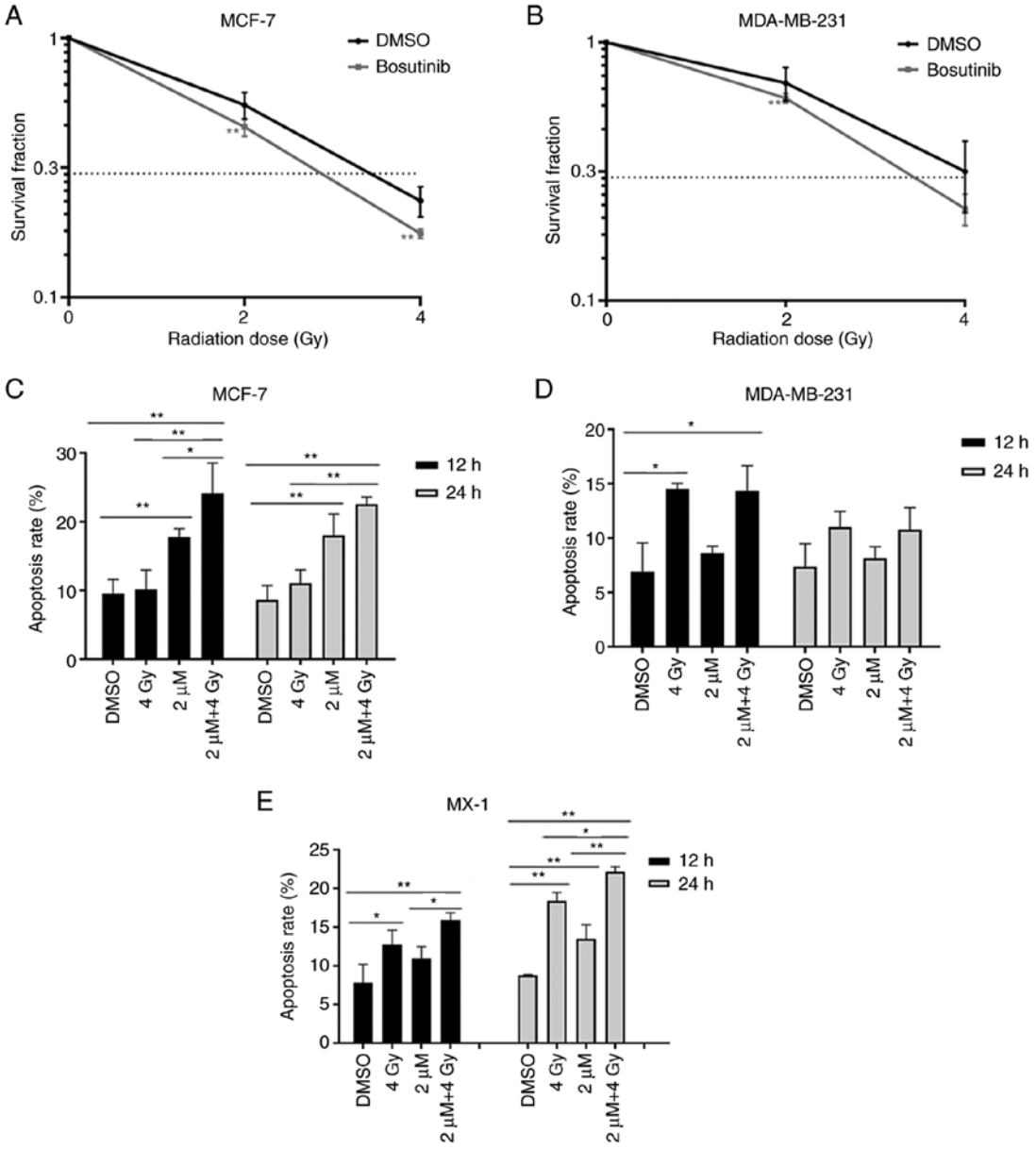

Figure 4. Bosutinib sensitizes cells to ionizing radiation (IR). (A and B) Sensitization of MCF-7 and MDA-MB-231 cells to γ-ray irradiation by bosutinib. (C-E) Effect of bosutinib on apoptosis induced by γ-ray irradiation in (C) MCF-7 cells, (D) MDA-MB-231 cells, and (E) MX-1 cells. Survival fractions were analyzed after treatment with 2 μM of bosutinib for 24 h followed by irradiation with doses of 0, 2 or 4 Gy. For the apoptosis assays, the cells were pre-treated with 2 μM of bosutinib for 24 h, followed by irradiation. Apoptosis rates represented the sum of both early and late apoptosis. Points show average, error bars show means ± standard deviations of three independent experiments. *P<0.05, **P<0.01.

The IC_{50} of bosutinib in MCF-7 and MDA-MB-231 cells were 5.4±3.63 μM and 3.2±0.07 μM, respectively. MX-1 cells were much more sensitive to bosutinib than the other two cell lines at concentrations of 0.5 and 1.0 μM (Fig. 3D).

Colony formation assays were conducted in MDA-MB-231 and MCF-7 cells. Cell proliferation in the two cell lines was inhibited by increasing concentrations of bosutinib (Fig. 3E and F). MDA-MB-231 cells were more sensitive to bosutinib than MCF-7 cells (Fig. 3F).

Bosutinib increases the radiosensitivity of breast cancer cells. Clonogenic assays were used to examine the radiosensitivity of MCF-7 and MDA-MB-231 cells. The cells were treated with 2 μM bosutinib for 24 h, then exposed to 2 or 4 Gy of γ-rays. Survival fractions (SF) following 2-Gy irradiation were 55.18 and 69.64% in MCF-7 and MDA-MB-231 cells, respectively. SF following 4-Gy irradiation were 23.56 and 31.64% in MCF-7 and MDA-MB-231 cells, respectively. Exposure to γ-rays alone killed breast cancer cells, and the viability rates decreased by 44.82 and 30.36% following 2-Gy irradiation in MCF-7 and MDA-MB-231 cells, respectively. After 4-Gy irradiation, the viability rates were further reduced by 76.44 and 68.36%, respectively (Fig. 4A and B), suggesting that MDA-MB-231 cells were more resistant to radiation. Bosutinib alone decreased the viability rates of the two cell lines by approximately 40%. When the treatment with irradiation and bosutinib was applied, SF following 2-Gy irradiation were 27.4 and 36.79% in MCF-7 and MDA-MB-231 cells, respectively. SF following 4-Gy irradiation were 10.63 and 13.65% in MCF-7 and MDA-MB-231 cells, respectively. Compared with

irradiation or bosutinib alone, the combined treatment reduced the viability of MCF-7 and MDA-MB-231 cells irradiated with 2 Gy from 55.18±6.51% to 27.4±0.74% and 69.64±10.28% to 36.79±2.05%, respectively, and irradiated with 4 Gy from 23.56±3.14% to 10.63±1.18% and 31.64±9.76% to 13.65±0.79%, respectively (Fig. S1). The combination indices (CI) in the two cell lines were calculated based on Chou-Talalay method with the tool CompuSyn. Inhibition rates of MCF-7 and MDA-MB-231 cells treated with bosutinib, radiation alone and their combinations (Table II) were used. The CI was 0.62 in MCF-7 cells treated with 2 μM bosutinib and 2-Gy radiation and 0.63 for 2 μM of bosutinib with 4-Gy of radiation. In MDA-MB-231 cells, the CI was 0.86 and 0.77 for 2 μM bosutinib with 2-Gy radiation and for 2 μM bosutinib with 4-Gy radiation, respectively. These findings indicated synergy between bosutinib and radiation, according to the Chou-Talalay method. Thus, bosutinib may notably improve the efficiency of radiation in killing cancer cells. These data suggested that the viability of breast cancer cells was reduced when bosutinib and irradiation were used in combination, highlighting bosutinib as a promising candidate radiosensitizer for its adjuvant effect to irradiation.

Apoptosis was detected in all three breast cancer cells at 12-96 h after irradiation. After 4-Gy irradiation alone, apoptosis was significantly increased at 12 h in MDA-MB-231 cells from 6.92 to 14.54% ($P<0.01$; Fig. 4D). In MX-1 cells, apoptosis increased significantly at 12 h from 7.83 to 12.77% ($P<0.05$) and at 24 h from 8.79 to 18.40% ($P<0.01$; Fig. 4E). This was not the case in MCF-7 cells (Fig. 4C). Treatment with bosutinib alone induced apoptosis in MCF-7 and MX-1 cells, but not in MDA-MB-231 cells. Apoptosis induced by the combined treatment of radiation and bosutinib in MCF-7 cells was 24.14% at 12 h and 22.56% at 24 h after irradiation. These apoptotic rates were much higher than those induced by radiation alone, which were nearly similar to the controls, suggesting an apparent radiosensitizing effect of bosutinib in MCF-7 cells (Fig. 4C). In MX-1 cells, the addition of bosutinib increased the rate of apoptosis from 12.77 to 15.90%, and from 18.40 to 22.15% at 12 and 24 h after irradiation, respectively, further indicating bosutinib as a potential adjuvant drug of irradiation (Fig. 4E). However, bosutinib did not promote apoptosis following irradiation in MDA-MB-231 cells, both at 12 and 24 h (Fig. 4D). Representative flow cytometry dot plots for apoptosis in the three cell lines are shown in Figs. S5-S7.

Bosutinib inhibits expression of eIF4G1. Western blot assays were conducted to detect the protein expression levels of eIF4G1 and its homolog eIF4G2 in all three breast cancer cell lines. The expression of eIF4G1 in MDA-MB-231 was lower than that in the other two cell lines (Fig. S2A and F). In MX-1 cells, eIF4G1 expression levels decreased in a dose-dependent manner following treatment with bosutinib (Fig. 5A and B). This decrease was apparent at the 12-h time-point at bosutinib concentrations of 1 and 5 μM, and at 24 h with concentrations ≥0.5 μM (Fig. 5B). However, eIF4G2 expression levels did not change markedly (Fig. 5G). In MCF-7 cells, eIF4G1 expression significantly decreased at 12 h at concentrations of ≥4 μM, and at 24 h at concentrations >1 μM (Fig. 5C and D). In MDA-MB-231 cells, eIF4G1 expression decreased significantly at >4 μM of bosutinib at both time-points (Fig. 5E and F). However, bosutinib did not affect the expression of eIF4G2 in MCF-7 and MDA-MB-231 cells (Fig. 5H and I).

Table II. Inhibition rates of different concentrations of bosutinib, different doses of radiation and their combinations in cell lines MCF-7 and MDA-MB-231.

Variable	MCF-7	MDA-MB-231
DMSO	0	0
Bosu 0.5 μM	14.37%	1.71%
Bosu 1 μM	23.93%	7.24%
Bosu 2 μM	39.77%	39.36%
Bosu 4 μM	36.53%	28.74%
Radi 2 Gy	44.82%	30.38%
Radi 4 Gy	76.44%	68.36%
2 μM+2 Gy	72.76%	63.21%
2 μM+4 Gy	89.37%	86.35%

'Bosu', bosutinib; 'Radi', γ-ray radiation.

Effect of bosutinib on the expression of DDR proteins. The effect of bosutinib on the expression of several DDR proteins was then evaluated. Bosutinib increased the levels of γH2AX expression, a biomarker of DNA double-strand breaks, or prolonged its vanishing effect in all three cell lines (Fig. 6), indicating increased DNA damage or reduced DNA repair efficiency (Fig. S4). The expression levels of other IR-induced DDR proteins were also measured. The expression levels of the ATM DNA repair protein were reduced after treatment with bosutinib, compared with before treatment, in MX-1 (Fig. 6A and B), MCF-7 (Fig. 6C and D) and MDA-MB-231 cells (Fig. 6E and F). In addition, the expression levels of DDR proteins XRCC4, ATRIP and GADD45A were also reduced in MDA-MB-231 and MCF-7 cells after bosutinib treatment with or without irradiation (Fig. S2B-E). Bosutinib did not alter the expression levels of PARP-1, Mre11, CDK1 and pCDK1 (Fig. S3).

Discussion

Advances in new physical and biological techniques in RT, including radiosensitization, are aimed at improving the clinical effect against cancer invasion and metastasis at a relatively low dose, with fewer adverse effects (40). Identifying effective radiosensitizers with a more favorable toxicity profile and understanding the underlying mechanism of radioresistance and radiosensitization is needed.

eIF4G1, the most abundant member of the eIF4G family, is a large scaffolding protein in the eIF4F complex, upon which ribosomes and eIFs assemble. Increased expression of eIF4G1 is associated with progression and metastasis of several cancer types (41). Thus, eIF4G1 has been proposed as a potential anticancer target.

Using computational methods, the present study investigated the repositioning opportunities of bosutinib, an oral, first-line, second-generation therapeutic drug approved for

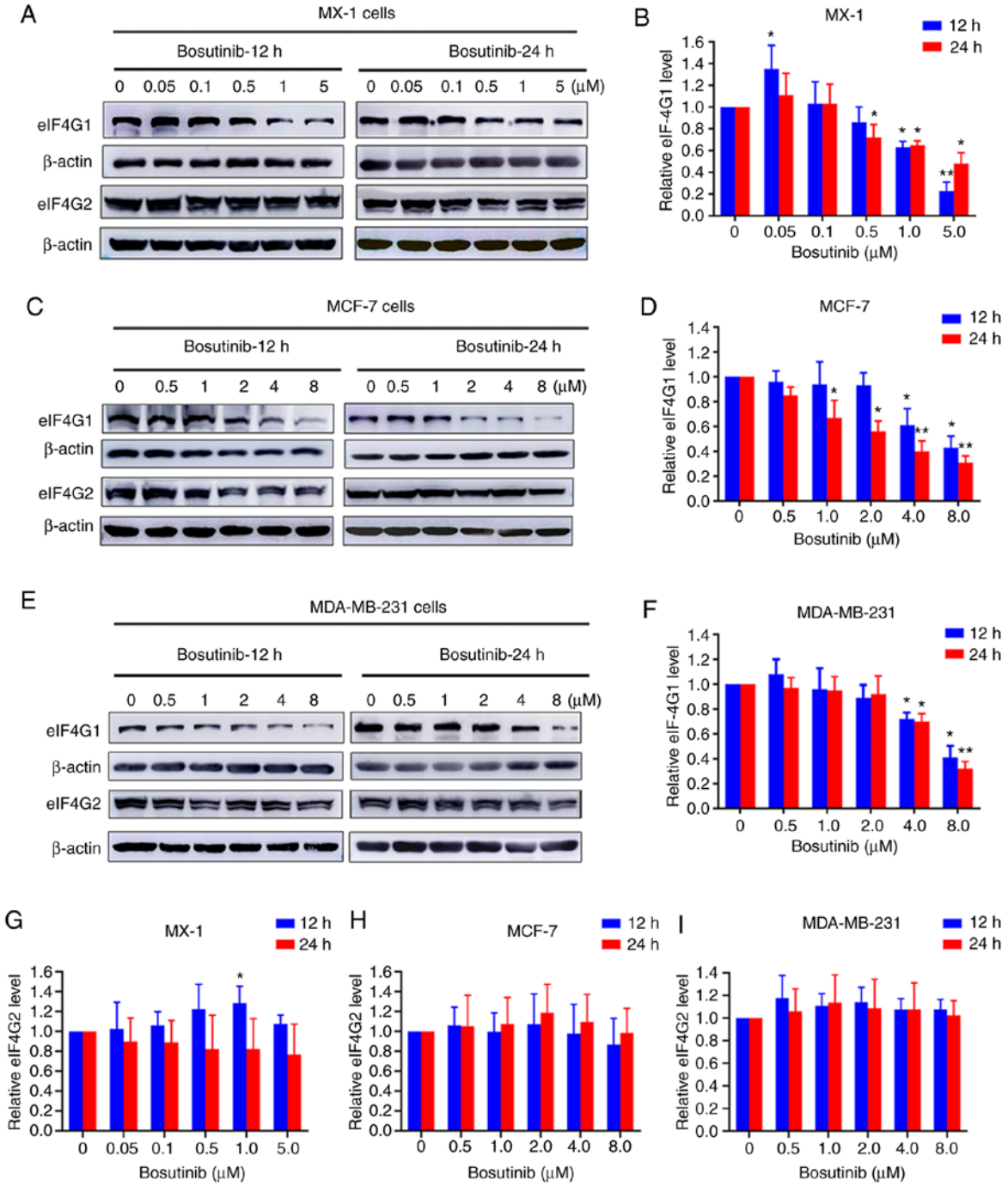

Figure 5. Effects of bosutinib on the expression of eIF4G1 and eIF4G2 in different cell lines. (A) The alterations of eIF4G1 and eIF4G2 expression in MX-1 cells after 12 and 24 h treatment with bosutinib at different concentrations. (B) Densitometry analysis of eIF4G1 expression in MX-1 cells treated with bosutinib for 12 and 24 h. (C) The alterations of eIF4G1 and eIF4G2 expression in MCF-7 cells after 12 and 24 h treatment with bosutinib at different concentrations. (D) Densitometry analysis of eIF4G1 expression in MCF-7 cells treated with bosutinib for 12 and 24 h. (E) The alterations of eIF4G1 and eIF4G2 expression in MDA-MB-231 cells after 12 and 24 h treatment with bosutinib at different concentrations. (F) Densitometry analysis of eIF4G1 expression in MDA-MB-231 cells treated with bosutinib for 12 and 24 h. (G) Densitometry analysis of eIF4G2 expression in MX-1 cells treated with bosutinib for 12 and 24 h. (H) Densitometry analysis of eIF4G2 expression in MCF-7 cells treated with bosutinib for 12 and 24 h. (I) Densitometry analysis of eIF4G2 expression in MDA-MB-231 cells treated with bosutinib for 12 and 24 h. The relative expression levels of the proteins were expressed as the ratio of hybridization gray values of the tested proteins and the loading control β-active, with normalized by the data of DMSO mock control samples. The data were expressed as the mean ± standard deviation from four independent experiments. *P<0.05, **P<0.01.

the treatment of newly diagnosed chronic myelogenous leukemia (42), as a new sensitizer for RT. The gene expression signature of bosutinib was compared with that of eIF4G1-silenced breast cancer cells in order to determine whether this drug could improve the sensitivity of the breast cancer cells to irradiation. The regulatory role of bosutinib in radiosensitivity and the mechanism underlying the effect of eIF4G1 in DNA double-strand break repair following IR were also examined.

The results indicated that the rates of apoptosis following RT in MCF-7 cells was lower compared with the two other cell lines. The order of sensitivity to higher concentrations

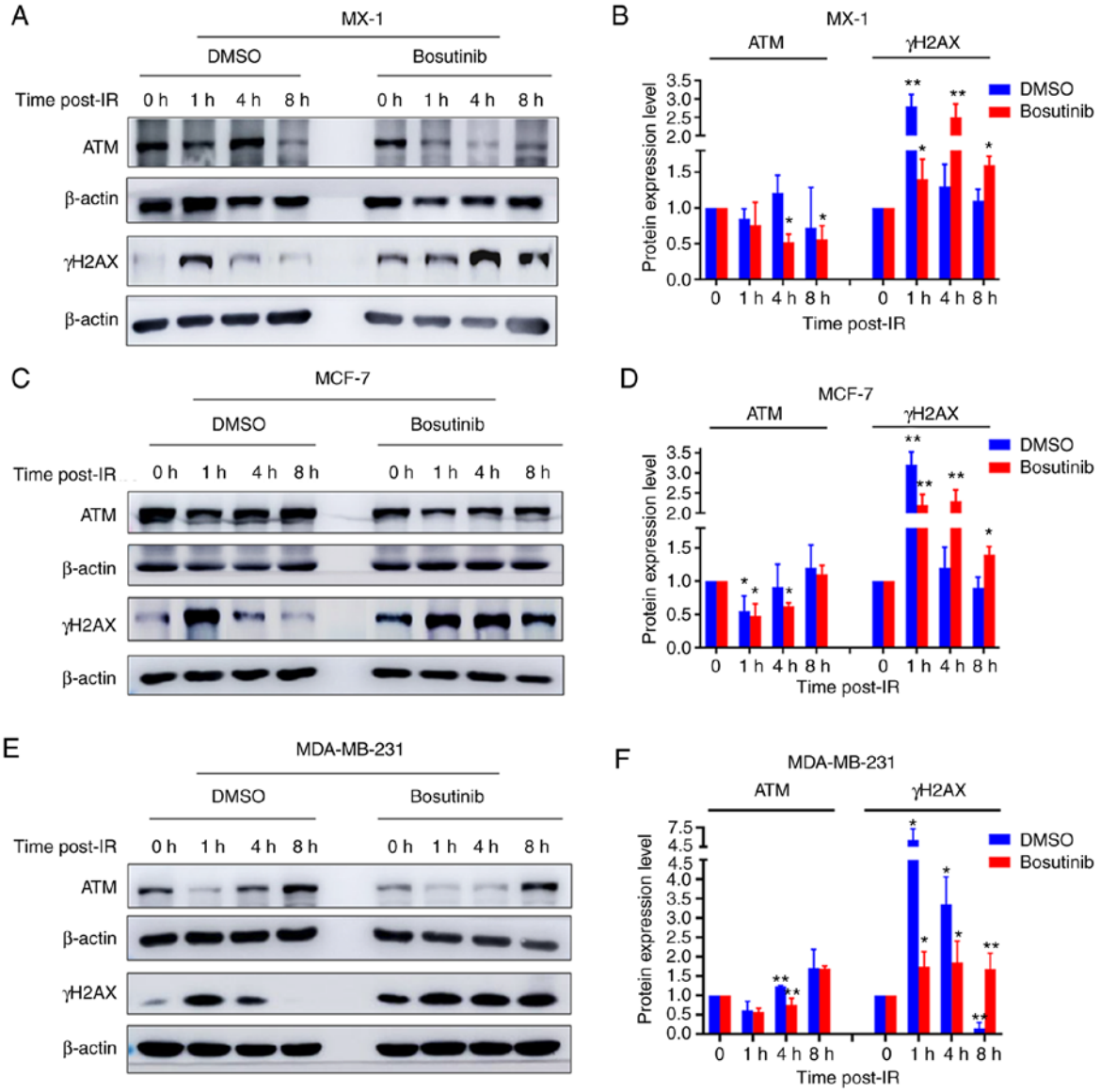

Figure 6. Effects of bosutinib on the expression of DNA damage response (DDR) proteins. (A) Western blotting of ATM and γH2AX expression in MX-1 cells after the indicated treatment. (B) Densitometry analysis of ATM and γH2AX expression in MX-1 cells. (C) Western blotting of ATM and γH2AX expression in MCF-7 cells after the indicated treatment. (D) Densitometry analysis of ATM and γH2AX expression in MCF-7 cells. (E) Western blotting of ATM and γH2AX expression in MDA-MB-231 cells after the indicated treatment. (F) Densitometry analysis of ATM and γH2AX expression in MDA-MB-231 cells. The cells were treated with 2 μM of bosutinib for 24 h, then irradiated with 4 Gy γ-ray. The protein expression levels were expressed as the ratio of hybridization signal gray values of the tested proteins and the loading control β-active, with normalized by the data of mock control samples. The data were expressed as the mean ± standard deviation from three independent experiments. *P<0.05, **P<0.01.

of bosutinib among the three breast cancer cell lines was: MX-1 > MDA-MB-231 > MCF-7 cells. Apoptosis was not evidently observed in bosutinib-treated MDA-MB-231 cells, with or without irradiation; thus, cell killing may be attributed to other mechanisms of cell death, such as autophagy (41-43), lysosomal membrane permeabilization (46) and cell cycle arrest (47). However, radiation and bosutinib combined significantly enhanced cell killing. Administration of bosutinib efficiently functioned at relatively low doses of both radiation and the drug, which may result in lower toxicity in normal tissues in the clinical setting.

Furthermore, the present findings also indicated that bosutinib inhibited eIF4G1 expression in all three cell lines in a dose-dependent manner. Importantly, bosutinib also inhibited the expression of several DDR-associated proteins by suppressing eIF4G1. This could represent a major cause of radiosensitization through eIF4G1 targeting (26). Consequently, the efficiency of DNA damage repair was reduced, as evidenced by the prolonged quenching effect of γH2AX. The mechanism of radiosensitization mediated by bosutinib could primarily be associated with eIF4G1. Thus, the present study highlights the effectiveness of the LINCS gene expression signature strategy in identifying novel applications of old drugs.

Recent studies have suggested that cancer patients who have undergone RT may be at increased risk of non-cancer diseases induced by late effects of radiation, such as cardiovascular diseases (48) and stroke (49). A comprehensive analysis demonstrated that, compared with other new-generation tyrosine kinase inhibitors, the incidence of vascular and cardiac treatment-associated adverse events in patients receiving

bosutinib were markedly lower, even after long-term treatment (50). Therefore, the addition of bosutinib would not increase the risk of cardiotoxicity.

Overall, the present study described a powerful approach to the identification of radiosensitizer candidates, based on rational computational drug repositioning. The findings on the mechanism of action of bosutinib in DDR may provide insight into gene regulation in IR-induced cellular damage. However, further *in vivo* experiments are needed to better understand the mechanisms that could overcome radioresistance in breast cancer cells. Advances in the development of effective radiosensitizers and further studies into the mechanism underlying the regulatory roles of genes involved in IR-induced damage may lead to improved therapeutic applications that could address radioresistance in cancer therapy.

In conclusion, using computational methods, the present study suggested that bosutinib, an FDA-approved drug, may be a potential radiosensitizer for breast cancer therapy. Experimental evidence also validated these results and suggested that eIF4G1 silencing resulted in the downregulation of the DDR proteins, thereby enhancing radiosensitivity in breast cancer cells. Thus, bosutinib is a potential candidate radiosensitizer for breast cancer therapy.

Acknowledgements

Not applicable.

Funding

The present was supported by the National Key Basic Research Program (973 Program) of MOST, China (grant no. 2015CB910601), the National Natural Science Foundation of China (grant nos. 11705283, 81530085 and 31870847), and the Young Elite Scientists Sponsorship Program of CAST (grant no. CSTQT2017003).

Availability of data and materials

The datasets used and/or analyzed during the current study are available from the corresponding author on reasonable request.

Authors' contributions

PZ and HG conceived and designed the study. SH, DX, PZ, XL, XY, BH and HG contributed to the concept, design and definition of the intellectual content of this study. DX and XY contributed to the data acquisition, calculation and statistical analyses. SH, XL and BH contributed to the experimental studies and statistical analyses. PZ and DX contributed to preparation and review of the manuscript. All authors read and approved the final manuscript.

Ethics approval and consent to participate

Not applicable.

Patient consent for publication

Not applicable.

Competing interests

The authors declare that they have no competing interests.

References

1. Bernier J: Precision medicine for early breast cancer radiotherapy: Opening up new horizons? Crit Rev Oncol Hematol 113: 79-82, 2017.
2. Bennett MH, Feldmeier J, Smee R and Milross C: Hyperbaric oxygenation for tumour sensitisation to radiotherapy. Cochrane Database Syst Rev 11: CD005007, 2012.
3. Schütze A, Vogeley C, Gorges T, Twarock S, Butschan J, Babayan A, Klein D, Knauer SK, Metzen E, Müller V, *et al*: RHAMM splice variants confer radiosensitivity in human breast cancer cell lines. Oncotarget 7: 21428-21440, 2016.
4. Huang RX and Zhou PK: DNA damage response signaling pathways and targets for radiotherapy sensitization in cancer. Signal Transduct Target Ther 5: 60, 2020.
5. Lai Y, Yu X, Lin X and He S: Inhibition of mTOR sensitizes breast cancer stem cells to radiation-induced repression of self-renewal through the regulation of MnSOD and Akt. Int J Mol Med 37: 369-377, 2016.
6. Silvera D, Formenti SC and Schneider RJ: Translational control in cancer. Nat Rev Cancer 10: 254-266, 2010.
7. Peretz S, Jensen R, Baserga R and Glazer PM: ATM-Dependent expression of the insulin-like growth factor-I receptor in a pathway regulating radiation response. Proc Natl Acad Sci USA 98: 1676-1681, 2001.
8. Luo YM, Xia NX, Yang L, Li Z, Yang H, Yu HJ, Liu Y, Lei H, Zhou FX, Xie CH, *et al*: CTC1 increases the radioresistance of human melanoma cells by inhibiting telomere shortening and apoptosis. Int J Mol Med 33: 1484-1490, 2014.
9. Dolman MEM, van der Ploeg I, Koster J, Bate-Eya LT, Versteeg R, Caron HN and Molenaar JJ: DNA-Dependent protein kinase as molecular target for radiosensitization of neuroblastoma cells. PLoS One 10: e0145744, 2015.
10. Rachmadi L, Siregar NC, Kanoko M, Andrijono A, Bardosono S, Suryandari DA, Sekarutami SM and Hernowo BS: Role of cancer stem cell, apoptotic factor, DNA repair, and telomerase toward radiation therapy response in stage IIIB cervical cancer. Oman Med J 34: 224-230, 2019.
11. Yu CC, Huang H, Hung SK, Liao HF, Lee CC, Lin HY, Li SC, Ho HC, Hung CL and Su YC: AZD2014 radiosensitizes oral squamous cell carcinoma by inhibiting AKT/mTOR axis and inducing G1/G2/M cell cycle arrest. PLoS One 11: e0151942, 2016.
12. Gewirtz DA: The four faces of autophagy: Implications for cancer therapy. Cancer Res 74: 647-651, 2014.
13. Khoshinani HM, Afshar S and Najafi R: Hypoxia: A double-edged sword in cancer therapy. Cancer Invest 34: 536-545, 2016.
14. Saenko YV, Mastilenko AV, Glushchenko ES, Antonova AV and Svekolkin VP: Inhibition of mitochondrial voltage-dependent anion channels increases radiosensitivity of K562 leukemic cells. Bull Exp Biol Med 161: 104-107, 2016.
15. Baro M, Sambrooks CL, Quijano A, Saltzman WM and Contessa J: Oligosaccharyltransferase inhibition reduces receptor tyrosine kinase activation and enhances glioma radiosensitivity. Clin Cancer Res 25: 784-795, 2019.
16. Segawa T, Fujii Y, Tanaka A, Bando SI, Okayasu R, Ohnishi K and Kubota N: Radiosensitization of human lung cancer cells by the novel purine-scaffold Hsp90 inhibitor, PU-H71. Int J Mol Med 33: 559-564, 2014.
17. Zhang L, Yoo S, Dritschilo A, Belyaev I and Soldatenkov V: Targeting ku protein for sensitizing of breast cancer cells to DNA-damage. Int J Mol Med 14: 153-159, 2004.
18. Zhang F, Fan B and Mao L: Radiosensitizing effects of cyclocarya paliurus polysaccharide on hypoxic A549 and H520 human non-small cell lung carcinoma cells. Int J Mol Med 44: 1233-1242, 2019.
19. Chang L, Graham PH, Hao J, Ni J, Bucci J, Cozzi PJ, Kearsley JH and Li Y: PI3K/Akt/mTOR pathway inhibitors enhance radiosensitivity in radioresistant prostate cancer cells through inducing apoptosis, reducing autophagy, suppressing NHEJ and HR repair pathways. Cell Death Dis 5: e1437, 2014.
20. Boguski MS, Mandl KD and Sukhatme VP: Drug discovery. Repurposing with a difference. Science 324: 1394-1395, 2009.
21. Rasheed S, Sánchez SS, Yousuf S, Honoré SM and Choudhary MI: Drug repurposing: In-vitro anti-glycation properties of 18 common drugs. PLoS One 13: e0190509, 2018.

22. Amsberg GK and Schafhausen P: Bosutinib in the management of chronic myelogenous leukemia. Biologics 7: 115-122, 2013.
23. Amsberg GKV and Brümmendorf TH: Novel aspects of therapy with the dual src and abl kinase inhibitor bosutinib in chronic myeloid leukemia. Expert Rev Anticancer Ther 12: 1121-1127, 2012.
24. Lee JH, Choi SI, Kim RK, Cho EW and Kim IG: Tescalcin/c-Src/IGF1Rβ-mediated STAT3 activation enhances cancer stemness and radioresistant properties through ALDH1. Sci Rep 8: 10711, 2018.
25. Cammarata FP, Torrisi F, Forte GI, Minafra L, Bravatà V, Pisciotta P, Savoca G, Calvaruso M, Petringa G, Cirrone GA, *et al*: Proton therapy and src family kinase inhibitor combined treatments on U87 human glioblastoma multiforme cell line. Int J Mol Sci 20: 4745, 2019.
26. Badura M, Braunstein S, Zavadil J and Schneider RJ: DNA damage and eIF4G1 in breast cancer cells reprogram translation for survival and DNA repair mRNAs. Proc Natl Acad Sci USA 109: 18767-18772, 2012.
27. Keenan AB, Jenkins SL, Jagodnik KM, Koplev S, He E, Torre D, Wang Z, Dohlman AB, Silverstein MC, Lachmann A, *et al*: The library of integrated network-based cellular signatures NIH program: System-Level cataloging of human cells response to perturbations. Cell Syst 6: 13-24, 2018.
28. Ritchie ME, Phipson B, Wu D, Hu Y, Law CW, Shi W and Smyth GK: Limma powers differential expression analyses for RNA-sequencing and microarray studies. Nucleic Acids Res 43: e47, 2015.
29. Subramanian A, Tamayo P, Mootha VK, Mukherjee , Ebert BL, Gillette MA, Paulovich A, Pomeroy SL, Golub TR, Lander ES and Mesirov JP: Gene set enrichment analysis: A knowledge-based approach for interpreting genome-wide expression profiles. Proc Natl Acad Sci USA 102: 15545-15550, 2005.
30. Pfeffer RM: Radiotherapy for breast cancer: Curing the cancer while protecting the heart. Isr Med Assoc J 20: 582-583, 2018.
31. Taylor CW and Kirby AM: Cardiac side-effects from breast cancer radiotherapy. Clin Oncol (R Coll Radiol) 27: 621-629, 2015.
32. Tarpley M, Abdissa TT, Johnson GL and Scott JE: Bosutinib reduces the efficacy of dasatinib in triple-negative breast cancer cell lines. Anticancer Res 34: 1629-1635, 2014.
33. Tan DSW, Haaland B, Gan JM, Tham SC, Sinha I, Tan EH, Lim KH, Takano A, Krisna SS, Thu MM, *et al*: Bosutinib inhibits migration and invasion via ACK1 in KRAS mutant non-small cell lung cancer. Mol Cancer 13: 13, 2014.
34. Wie SM, Wellberg E, Karam SD and Reyland ME: Tyrosine kinase inhibitors protect the salivary gland from radiation damage by inhibiting activation of protein kinase C-δ. Mol Cancer Ther 16: 1989-1998, 2017.
35. Wenzel T, Büch T, Urban N, Weirauch U, Schierle K, Aigner A, Schaefer M and Kalwa H: Restoration of MARCKS enhances chemosensitivity in cancer. J Cancer Res Clin Oncol 146: 843-858, 2020.
36. Chou TC: Drug combination studies and their synergy quantification using the chou-talalay method. Cancer Res 70: 440-446, 2010.
37. Ellegaard AM, Groth-Pedersen L, Oorschot V, Klumperman J, Kirkegaard T, Nylandsted J and Jäättelä M: Sunitinib and SU11652 inhibit acid sphingomyelinase, destabilize lysosomes, and inhibit multidrug resistance. Mol Cancer Ther 12: 2018-2030, 2013.
38. Evelyn CR, Lisabeth EM, Wade SM, Haak AJ, Johnson CN, Lawlor ER and Neubig RR: Small-Molecule inhibition of Rho/MKL/SRF transcription in prostate cancer cells: Modulation of cell cycle, er stress, and metastasis gene networks. Microarrays (Basel) 5: 13, 2016.
39. Wainberg ZA, Alsina M, Soares HP, Braña I, Britten CD, Conte GD, Ezeh P, Houk B, Kern KA, Leong S, *et al*: A multi-arm phase I study of the PI3K/mTOR inhibitors PF-04691502 and gedatolisib (PF-05212384) plus irinotecan or the MEK inhibitor PD-0325901 in advanced cancer. Target Oncol 12: 775-785, 2017.
40. Hamilton DG, Bale R, Jones C, Fitzgerald E, Khor R, Knight K and Wasiak J: Impact of tumour bed boost integration on acute and late toxicity in patients with breast cancer: A systematic review. Breast 27: 126-135, 2016.
41. Jaiswal PK, Koul S, Shanmugam PST and Koul HK: Eukaryotic translation initiation factor 4 gamma 1 (eIF4G1) is upregulated during prostate cancer progression and modulates cell growth and metastasis. Sci Rep 8: 7459, 2018.
42. Gourd E: Bosutinib more effective than imatinib in CML. Lancet Oncol 18: e716, 2017.
43. Hu MB, Zhang JW, Gao JB, Qi YW, Gao Y, Xu L, Ma Y and Wei ZZ: Atorvastatin induces autophagy in MDA-MB-231 breast cancer cells. Ultrastruct Pathol 42: 409-415, 2018.
44. Chang CH, Bijian K, Wernic D, Su J, da Silva SD, Yu H, Qiu D, Asslan M and Alaoui-Jamali MA: A novel orally available seleno-purine molecule suppresses triple-negative breast cancer cell proliferation and progression to metastasis by inducing cytostatic autophagy. Autophagy 15: 1376-1390, 2019.
45. Lin SC, Chu PY, Liao WT, Wu MY, Tsui KH, Lin LT, Huang CH, Chen LL and Li CJ: Glycyrrhizic acid induces human MDA-MB-231 breast cancer cell death and autophagy via the ROS-mitochondrial pathway. Oncol Rep 39: 703-710, 2018.
46. Noguchi S, Shibutani S, Fukushima K, Mori T, Igase M and Mizuno T: Bosutinib, an SRC inhibitor, induces caspase-independent cell death associated with permeabilization of lysosomal membranes in melanoma cells. Vet Comp Oncol 16: 69-76, 2018.
47. Nam AR, Kim JW, Park JE, Bang JH, Jin MH, Lee KH, Kim TY, Han SW, Im SA, Kim TY, *et al*: Src as a therapeutic target in biliary tract cancer. Mol Cancer Ther 15: 1515-1524, 2016.
48. Weberpals J, Jansen L, Müller OJ and Brenner H: Long-Term heart-specific mortality among 347 476 breast cancer patients treated with radiotherapy or chemotherapy: A registry-based cohort study. Eur Heart J 39: 3896-3903, 2018.
49. Huang R, Zhou Y, Hu S, Ren G, Cui F and Zhou PK: Radiotherapy exposure in cancer patients and subsequent risk of stroke: A systematic review and meta-analysis. Front Neurol 10: 233, 2019.
50. Cortes JE, Khoury HJ, Kantarjian H, Brümmendorf TH, Mauro MJ, Matczak E, Pavlov D, Aguiar JM, Fly KD, Dimitrov S, *et al*: Long-Term evaluation of cardiac and vascular toxicity in patients with philadelphia chromosome-positive leukemias treated with bosutinib. Am J Hematol 91: 606-616, 2016.